Anal. Chem. **2003,** *75,* 5328−5335

Dual-Function Microanalytical Device by In Situ Photolithographic Grafting of Porous Polymer Monolith: Integrating Solid-Phase Extraction and Enzymatic Digestion for Peptide Mass Mapping

Dominic S. Peterson,[†] Thomas Rohr,[†] Frantisek Svec,[†,‡] and Jean M. J. Fréchet*[,†,‡]

Materials Sciences Division, E. O. Lawrence Berkeley National Laboratory, Berkeley, California 94720-8139, and Department of Chemistry, University of California, Berkeley, California 94720-1460

Microfluidic devices with a dual function containing both a solid-phase extractor and an enzymatic microreactor have been prepared, and their operation has been demonstrated. The devices were fabricated from a 25-mm-long porous poly(butyl methacrylate-*co*-ethylene dimethacrylate) monolith prepared within a 50-μm-i.d. capillary. This capillary with a pulled 9−12-μm needle tip was used as a nanoelectrospray emitter coupling the device to a mass spectrometer. Photografting with irradiation through a mask was then used to selectively functionalize a 20-mm-long portion of the monolith, introducing reactive poly(2-vinyl-4,4-dimethylazlactone) chains to enable the subsequent attachment of trypsin, thereby creating an enzymatic microreactor with high proteolytic activity. The other 5 mm of unmodified hydrophobic monolith served as micro solid-phase extractor (μSPE). The dual-function devices were used in two different flow directions; concentration of myoglobin that was absorbed from its dilute solution, followed by elution and digestion or digestion, followed by concentration. Operations in both directions afforded equal sequence coverage. Different volumes of myoglobin solution ranging from 2 to 20 μL were loaded on the device. Very high sequence coverages of almost 80% were achieved for the highest loading. Despite the very short length of the extractor unit, the device operated in the digest−solid-phase extraction direction also enabled the separation of peaks that mostly contained undigested protein and peptides.

Proteomics, which represents the next major target in the postgenomic era, is believed to facilitate the search for therapeutically significant proteins. Increasing activity in the area of proteomics makes the development of new techniques highly desirable.[1] Peptide-mass mapping that typically includes digestion with a proteolytic enzyme followed by MS analysis is one of the routine methods that currently seems best suited to determine both protein identity and posttranslational modifications.[2] Most of the current protocols include digestion with trypsin in solution.[3] The undesired autodigestion can be eliminated by immobilizing the proteolytic enzymes on a solid support.[4] Miniaturization appears to be critical in the field of proteomics,[5] and a number of microfluidic devices involving immobilized enzymes have been designed.[6]

Yet another challenge is to identify the proteins that are present at very low concentrations in analyte solutions. Therefore, some protocols include a preconcentration step using, for example, solid-phase extraction (SPE).[7] The compounds of interest are first adsorbed onto the surface of porous materials and later released

* Corresponding author. E-mail: frechet@cchem.berkeley.edu.
[†] Lawrence Berkeley National Laboratory.
[‡] University of California at Berkeley.

(1) (a) Hancock, W. S.; Wu, S. L.; Shieh, P. *Proteomics* **2002**, *2*, 352−359. (b) Dongre, A. R.; Opiteck, G.; Cosand, W. L.; Hefta, S. A. *Biopolymers* **2001**, *60*, 206−211. (c) Foret, F.; Preisler, J. *Proteomics* **2002**, *2*, 360−372.

(2) (a) Lazar, I. M.; Ramsey, R. S.; Ramsey, J. M. *Anal. Chem.* **2001**, *73*, 1733−1739. (b) Gevaert, K.; Vandekerckhove, J. *Electrophoresis* **2000**, *21*, 1145−1154.

(3) Wu, J.-T.; Huang, P.; Li, M. X.; Lubman, D. M. *Anal. Chem.* **1997**, *69*, 9, 2908−2913.

(4) (a) Moulin, C. In *Methods in Enzymology*; Colowick, S. P., Caplan, N. O., Eds.; Academic Press: New York, 1987. (b) Mansson, M. O.; Mosbach, K. *Methods Enzymol.* **1987**, *136*, 3−9. Nilsson, K.; Mosbach, K. *Methods Enzymol.* **1987**, *135*, 65−78. (c) Siegbahn, N.; Mansson, M. O.; Mosbach, K. *Methods Enzymol.* **1987**, *136*, 103−113. (d) Tischer, W.; Wedekind, F. *Top. Curr. Chem.* **1999**, 95−126. (e) Lalonde, J.; Margolin, A. In *Enzyme Catalysis in Organic Synthesis*, 2nd ed.; Drauz, K., Waldmann, H., Eds.; Wiley-VCH: New York, 2002; pp 163−184.

(5) Laurell, T.; Marko-Varga, G. *Proteomics* **2002**, *2*, 345−351.

(6) (a) Zhan, W.; Seong, G. H.; Crooks, R. M. *Anal. Chem.* **2002**, *74*, 4647−4652. (b) Seong, G. H.; Zhan, W.; Crooks, R. M. *Anal. Chem.* **2002**, *74*, 3372−3377. (c) Sakai-Kato, K.; Kato, M.; Toyo'oka, T. *Anal. Chem.* **2002**, *74*, 2943−2949. (d) Kato, M.; Sakai-Kato, K.; Matsumoto, N.; Toyo'oka, T. *Anal. Chem.* **2002**, *74*, 1915−1921. (e) Li, C. I.; Lin, Y. H.; Shih, C. L.; Tsaur, J. P.; Chau, L. K. *Biosens. Bioelectron.* **2002**, *17*, 323−330. (f) Park, C. B.; Clark, D. S. *Biotechnol. Bioeng.* **2002**, *78*, 229−235. (g) Sato, K.; Tokeshi, M.; Odake, T.; Kimura, H.; Ooi, T.; Nakao, M.; Kitamori, T. *Anal. Chem.* **2000**, *72*, 1144−1147. (h) Blackburn, R. K.; Anderegg, R. J. *J. Am. Soc. Mass Spectrom.* **1997**, *8*, 483−494. (i) L'Hostis, E.; Michel, P. E.; Fiaccabrino, G. C.; Strike, D. J.; de Rooij, N. F.; Koudelka-Hep, M. *Sens. Actuators, B* **2000**, *64*, 156−162. (j) Wang, C.; Oleschuk, R.; Ouchen, F.; Li, J. J.; Thibault, P.; Harrison, D. J. *Rapid Commun. Mass Spectrom.* **2000**, *14*, 1377−1383. (k) Cooper, J. W.; Chen, J.; Li, Y.; Lee, C. S. *Anal. Chem.* **2003**, *75*, 1067−1074.

(7) (a) Sarrión, M. N.; Santos, F. J.; Galceran, M. T. *Anal. Chem.* **2000**, *72*, 4865−4873. (b) Thurman; E. M.; Mills, M. S. *Solid-Phase Extraction. Principles and Practice*; Wiley: New York, 1998. (c) Masqué, N.; Marce, R. M.; Borrull, F.; Cormack, P. A. G.; Sherrington, D. C. *Anal. Chem.* **2000**, *72*, 4122−4126. (d) Ferrer, I.; Lanza, F.; Tolokan, A.; Horvath, V.; Sellergren, B.; Horvai, G.; Barcelo, D. *Anal. Chem.* **2000**, *72*, 3934−3941. (e) Li, N. Q.; Lee, H. K. *Anal. Chem.* **2000**, *72*, 3077−3084. (f) Shamsipur, M.; Ghiasvand, A. R.; Yamini, Y. *Anal. Chem.* **1999**, *71*, 4892−4895. (g) Li, N. Q.; Lee, H. K. *Anal. Chem.* **1997**, *69*, 5193−5199.

10.1021/ac034108j CCC: $25.00
Published on Web 08/29/2003

by elution with a stronger solvent in a concentrated band.[8] Specifically designed SPE devices have also been used to eliminate interfering compounds.[7]

New functional microdevices, such as nanoelectrospray needles packed with a beaded chromatographic stationary phase, also vastly simplify the use of mass spectrometers with electrospray ionization (ESI) for the detection and identification of proteins and peptides in proteomic research.[9] Moore[10] adapted our earlier work[11] and used hydrophobic porous polymer monolith in the separations of proteins and peptides combined with MS detection. Alternatively, our monolithic frits[12] were in used a needle packed with a HPLC stationary phase.[13] We have also demonstrated recently the use of reactive monoliths directly polymerized in capillaries as supports for trypsin immobilization and their use in the digestion of proteins followed by MS determination of the peptides.[14] These examples clearly document the versatility of the monolithic polymers that we introduced in the early 1990s[15] and used in a number of applications.[14−16] To avoid reoptimization of both chemistry and the preparation procedure, we recently developed a new two step approach to well-defined monoliths with a wide variety of surface chemistries based on photografting.[17,18] This technique also enables the simple preparation of monoliths with cocontiguous chemistries by using photomasks.

Following our recent success with individually developed microfluidic devices, we have now used the unique features of our photografting procedure[17] that enables spatial control of surface chemistry to combine both SPE and enzymatic digestion in a single dual-function microdevice that may find applications in the detection of protein contaminants in our environment and in the detection of biological warfare agents. Since this device is prepared directly in the nanoelectrospray needle, interfacing with a mass spectrometer is a very simple process.

EXPERIMENTAL SECTION

Materials. Butyl methacrylate (99%, BuMA), ethylene dimethacrylate (98%, EDMA), 2-hydroxyethyl methacrylate (97%, HEMA), 2,2-dimethoxy-2-phenyl acetophenone (99%, DMAP), tris(hydroxymethyl)aminomethane (Tris), sodium sulfate, benzamidine, 1-decanol, and 3-(trimethoxysilyl)propyl methacrylate (98%) were purchased form Aldrich (Milwaukee, WI). *tert*-Butyl alcohol (99.7%, *t*BuOH) was obtained from J. T. Baker (Phillispburg, NJ). Trypsin from bovine pancreas, *N*-α-benzoyl-L-arginine ethyl ester (BAEE), equine myoglobin, and ethanolamine (98%) were from Sigma (St. Louis, MO), and BODIPY-labeled casein was from Molecular Probes (Eugene, OR). UV-transparent 50-μm-i.d., 360-μm-o.d. fused-silica tubing was purchased from Polymicro Technologies (Phoenix, AZ). 2-Vinyl-4,4-dimethylazlactone (VAL) was a gift from the 3M Company (St. Paul, MN) and was distilled prior to use. EDMA, BuMA, and HEMA were passed through basic alumina, followed by a distillation under reduced pressure. All other reagents were used as received.

Caution: 2-Vinyl-4,4-dimethylazlactone, several methacrylates, and solvents are known sensitizing agents. Benzamidine is an irritant. Proper precautions should be taken during the physical handling of these materials.

Nanospray Needles. The electrospray needles were made in-house from a fused-silica capillary using a P-2000 micropipet puller equipped with a CO_2 laser (Sutter Instruments, Novato, CA). The tips had a 1−2-mm-long narrowed region and an orifice of 10.5 ± 1.5 μm (n = 6, measured using SEM).

Monolithic Polymer. The internal wall surface of the capillaries was first vinylized to enable covalent attachment of the monolith to the walls.[19] The capillaries were rinsed with acetone and water; activated with a 0.2 mol/L sodium hydroxide for 30 min,; washed with water, followed by 0.2 mol/L HCl for 30 min; and finally, rinsed with ethanol. A 20% solution of 3-(trimethoxysilyl)propyl methacrylate in 95% ethanol with its pH adjusted to 5 using acetic acid was then pumped through the capillary for 1 h. Following washing with ethanol and drying in a stream of nitrogen, the functionalized capillaries were left at room temperature for 24 h.

Using capillary action, these capillaries were filled with a polymerization mixture (Table 1) to a length of 20 mm for devices containing only the enzymatic reactor (preliminary testing) and to 25 mm for devices containing both the solid-phase extractor and microreactor. An Oriel deep-UV illumination instrument (series 8700, Stratford, CT) fitted with a 500-W HgXe lamp was used to initiate the polymerization. The irradiation power of this lamp was adjusted to 15.0 mW/cm^2. Polymerization was completed

(8) (a) Doucette, A.; Craft, D.; Li, L. *Anal. Chem.* **2000**, *72*, 3355−3362. (b) Craft, D.; Doucette, A.; Li, L. *J. Proteome Res.* **2002**, *1*, 537−547.

(9) (a) Andren, P. E.; Emmett, M. R.; Caprioli, R. M. *J. Am. Soc. Mass Spectrom.* **1994**, *5*, 867−869. (b) Gatlin, C. L.; Kleemann, G. R.; Hays, L. G.; Link, A. J.; Yates, J. R. *Anal. Biochem.* **1998**, *263*, 93−101. (c) Davis, M. T.; Stahl, D. C.; Hefta, S. A.; Lee, T. D. *Anal. Chem.* **1995**, *67*, 4549−4556. (d) Ishihama, Y.; Rappsilber, J.; Andersen, J. S.; Mann, M. *J. Chromatogr., A* **2002**, *979*, 233−239.

(10) Moore, R. E.; Licklider, L.; Schumann, D.; Lee, T. D. *Anal. Chem.* **1998**, *70*, 4879−4884.

(11) Wang, Q.; Svec, F.; Fréchet, J. M. J. *Anal. Chem.* **1993**, *65*, 2243−2248.

(12) Chen, J. R.; Zare, R. N.; Peters, E. C.; Svec, F.; Fréchet, J. M. J. *Anal. Chem.* **2001**, *73*, 1987−1992.

(13) Haskins, W. E.; Wang, Z. Q.; Watson, C. J.; Rostand, R. R.; Witowski, S. R.; Powell, D. H.; Kennedy, R. T. *Anal. Chem.* **2001**, *73*, 5005−5014.

(14) (a) Peterson, D. S.; Rohr, T.; Svec, F.; Fréchet, J. M. J. *Anal. Chem.* **2002**, *74*, 4081−4088. (b) Peterson, D. S.; Rohr, T.; Svec, F.; Fréchet, J. M. J. *J. Proteome Res.* **2002**, *1*, 563−568.

(15) (a) Svec, F.; Fréchet, J. M. J. *Anal. Chem.* **1992**, *64*, 820−822. (b) Svec, F.; Fréchet, J. M. J. *Science* **1996**, *273*, 205−211.

(16) (a) Tennikova, T. B.; Bleha, M.; Svec, F.; Almazova, T. V.; Belenkii, B. G. *J. Chromatogr.* **1991**, *555*, 97−107. (b) Lämmerhofer, M.; Peters, E. C.; Yu, C.; Svec, F.; Fréchet, J. M. J.; Lindner, W. *Anal. Chem.* **2000**, *72*, 4623−4628. (c) Hilder, E. F.; Svec, F.; Fréchet, J. M. J. *Electrophoresis* **2002**, *23*, 3934−3953. (d) Yu, C.; Svec, F.; Fréchet, J. M. J. *Electrophoresis* **2000**, *21*, 120−127. Yu, C.; Davey, M. H.; Svec, F.; Fréchet, J. M. J. *Anal. Chem.* **2001**, *73*, 5088−5096. (e) Viklund, C.; Ponten, E.; Glad, B.; Irgum, K.; Horsted, P.; Svec, F. *Chem. Mater.* **1997**, *9*, 463−471. (f) Fintschenko, Y.; Choi, W. Y.; Ngola, S. M.; Shepodd, T. J. *Fresenius' J. Anal. Chem.* **2001**, *371*, 174−181. (g) Ngola, S. M.; Fintschenko, Y.; Choi, W. Y.; Shepodd, T. J. *Anal. Chem.* **2001**, *73*, 849−856. (h) Shediac, R.; Ngola, S. M.; Throckmorton, D. J.; Anex, D. S.; Shepodd, T. J.; Singh, A. K. *J. Chromatogr., A* **2001**, *925*, 251−263. (i) Throckmorton, D. J.; Shepodd, T. J.; Singh, A. K. *Anal. Chem.* **2002**, *74*, 784−789. (j) Rohr, T.; Yu, C.; Davey, M. H.; Svec, F.; Fréchet, J. M. J. *Electrophoresis* **2001**, *22*, 3959−3967.

(17) (a) Rohr, T.; Hilder, E. F.; Donovan, J. J.; Svec, F.; Fréchet, J. M. J. *Macromolecules* **2003**, *36*, 1677−1684. (b) Rohr, T.; Ogletree, D. F.; Svec, F.; Fréchet, J. M. J. *Adv. Funct. Mater.* **2003**, *13*, 264−270.

(18) (a) Oster, G.; Shibata, O. *J. Polym. Sci.* **1957**, *26*, 233−234. (b) Rånby, B. *Makromol. Chem. Macromol. Symp.* **1992**, *63*, 55−67. (c) Rånby, B. *Mater. Res. Innovations* **1998**, *2*, 64−71. (d) Rånby, B.; Yang, W. T.; Tretinnikov, O. *Nucl. Instrum. Methods Phys. Res. B* **1999**, *151*, 301−305. (e) Rånby, B. *Int. J. Adhes. Adhes.* **1999**, *19*, 337−343. Yang, W. T.; Rånby, B. *J. Appl. Polym. Sci.* **1996**, *62*, 533−543. (f) Yang, W. T.; Rånby, B. *Polym. Bull.* **1996**, *37*, 89−96.

(19) Ericson, C.; Liao, J. L.; Nakazato, K.; Hjertén, S. *J. Chromatogr., A* **1997**, *767*, 33−41.

Table 1. Polymerization Mixtures and Reaction Conditions Used for the Preparation of Monolithic Supports and Porous Properties of Resulting Monoliths

polymerization mixture	A	B
ethylene dimethacrylate, wt %	16	20
butyl methacrylate, wt %	24	
2-hydroxyethyl methacrylate, wt %		12
2-vinyl-4,4-dihethylazlactone, wt %		8
1-decanol, wt %	43.3	60
cyclohexanol, wt %	16.7	
2,2-dimethoxy-2-phenylacetophenone[a]	1	1
polymerization time, min	10	10
temperature, °C	20	20
pore volume, mL/g	1.79	1.33
median pore diameter, μm	0.96	1.02
porosity, %	59.9	51.9
specific surface area, m^2/g	8.3	6.4

[a] Percentage of initiator with respect to monomers.

after 10 min of irradiation at a distance of 30 cm. For the preparation of monoliths in previously pulled needles, the butt end was immersed in the polymerization mixture, which was filled by capillary action. The emitter was then masked using opaque electrical tape and UV-irradiated for 3 min. The monoliths were then washed for 12 h using a pressurized flow of methanol delivered by a syringe pump (KD Scientific, New Hope, PA).

The weight of the monoliths prepared within the capillaries is not sufficient for porosimetry measurement. Therefore, we polymerized the same mixture in a thin larger-volume mold described elsewhere. [17] The porous properties of this monolith prepared in bulk were then determined using an Autopore III 9400 mercury intrusion porosimeter (Micromeritics, Norcross, GA). An ISI high-resolution analytical scanning electron microscope (Topcon, Japan) was used to obtain the SEM images.

Photografting of 4,4-Dimethyl-2-vinylazlactone. The degassed VAL solution was pumped through the monolith at a flow rate of 0.1 μL/min for 30 min. The photomask was prepared by painting the capillary with flat black enamel paint. In some cases, a 1.1-mm-thick borofloat glass wafer with a diameter of 100 mm (Precision Glass & Optics, Santa Ana, CA) was placed over the capillary to act as a filter. The capillary filled with the grafting mixture was then placed under the UV lamp and irradiated from a distance of 30 cm for the specified period of time. After the grafting was completed, the monoliths were washed with acetone at a flow rate of 0.1 μL/min for 12 h.

Immobilization of Trypsin and Assay of Enzymatic Activity. A procedure that we developed earlier was used to immobilize trypsin on the monoliths.[14] The enzymatic activity was determined with 20-mm-long microreactors (total volume of 39.3 nL) that did not contain the μSPE part. The activity of the free trypsin (32.4 μmol/min·mg) was determined using a standard procedure.[20] The activity of immobilized enzyme was assayed by pumping a solution of BAEE (15−230 mmol/L) in a 50 mmol/L Tris buffer (pH = 8.0) using a Waters CapLC system (Milford, MA) through the monolith at a flow rate of 3 μL/min with detection of the resulting products at 254 nm. The enzymatic activity was calculated by multiplying the flow rate by the conversion obtained from the difference in absorption between both blank and converted solutions.

Dual-Function Devices. These devices included a 20-mm-long microreactor (39.3 nL) and a 5-mm-long (10 nL) μSPE unit. Their function was tested by pumping a 19 pmol/μL myoglobin solution in a 10 mmol/L solution of ammonium acetate at a flow rate of 0.5 μL/min from an injection loop (2−20 μL, Upchurch, Oak Harbor, WA) attached to a Rheodyne injector (Rohnert Park, CA). One minute after all the desired volume of the protein was pumped through the device, the flow was switched, and the sample was released from the μSPE unit using 50 nL of pure acetonitrile or its mixtures with water. To compare the function of the dual-function device with that of the microreactor alone, the latter was connected to a commercial nanoelectrospray needle (New Objective, Woburn, MA), and 50 nL of the myoglobin solution was pumped through. ESI-MS spectra were collected using an orthogonal acceleration time-of-flight mass spectrometer, Micromass LCT (Manchester, U.K.), equipped with a Picoview nanospray interface (New Objective). All MS data were collected in the negative ion mode. The mass spectra of all samples were then compared against the protein digestion database (protein prospector, http://prospector.ucsf.edu/) to identify the digest and determine the sequence coverage.[21]

RESULTS AND DISCUSSION

Preparation of the Monolithic Microreactors. The compositions of the two polymerization mixtures used in this study for the in situ preparation of monolithic materials are shown in Table 1. Mixture A, used for the preparation of the generic monolith, contained EDMA and BuMA. Post functionalization of the pore surface of this monolith was then carried out. Mixture B was used to prepare a functionalized monolith by direct copolymerization of EDMA, HEMA, and VAL. Both types of monoliths exhibited similar pore sizes, thus enabling a direct comparison of the functional devices prepared by the two approaches.

Surface functionalization of monolith A was achieved by photografting VAL onto the pore surface. This versatile monomer[22] enables the formation of reactive polymer chains with azlactone functionalities that react with the amino and thiol groups of proteins to effect their efficient immobilization.[23] The extent of grafting, which affects the activity of the immobilized trypsin microreactor, depends on both the time of irradiation and the intensity of the UV light. The former is easy to control by on−off switching, and borofloat glass can be used as a simple filter to modulate the light intensity at the wavelength used to excite the benzophenone and trigger the grafting. Table 2 shows the effects of these variables on the kinetic parameters of immobilized trypsin (maximum velocity, V_{max}, and Michaelis constant, K_m) and compares them with those obtained for the copolymerized

(20) Rick, W. *Methods of Enzymatic Analysis*; Bergmeyer, H. U., Ed.; Academic Press: New York, 1965.

(21) Clauser, K. R.; Baker, P.; Burlingame, A. L. *Anal. Chem.* **1999**, *71*, 2871−82.

(22) Heilmann, S. M.; Rasmussen, J. K.; Krepski, L. R. *J. Polym. Sci., Polym. Chem.* **2001**, *39*, 3655−77.

(23) (a) Coleman, P. L.; Walker, M. M.; Milbrath, D. S.; Stauffer, D. M.; Rasmussen, J. K.; Krepski, L. R.; Heilmann, S. M. *J. Chromatogr.* **1990**, *512*, 345−63. (b) Rasmussen, J. K.; Heilmann, S. M.; Krepski, L. R.; Jensen, K. M.; Mickelson, J.; Johnson, K. Z.; Coleman, P. L.; Milbrath, D. S.; Walker, M. M. *React. Polym.* **1992**, *16*, 199−212. (c) Xie, S. F.; Svec, F.; Fréchet, J. M. J. *Biotechnol. Bioeng.* **1999**, *62*, 30−35.

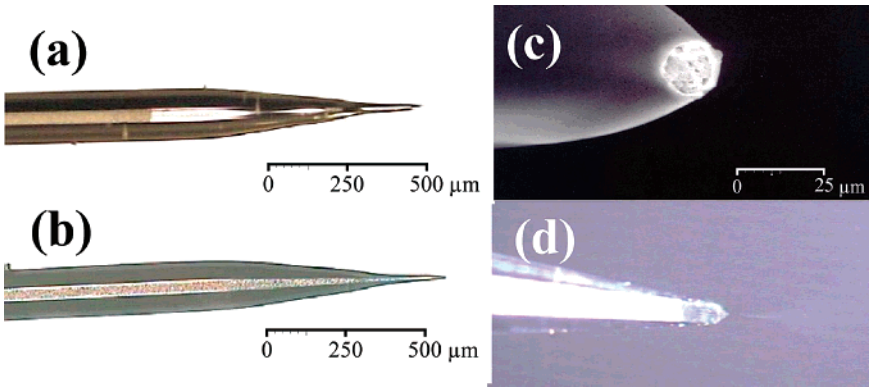

Figure 1. Optical micrograph of monolith prepared in capillary prior to pulling the nanoelectrospray needle (a), optical (b) and SEM micrograph (c) of monolith prepared directly in a needle, and electrospray beam generated from the tip containing a monolith (d).

Table 2. Effect of Grafting Conditions on Activity and Backpressure of Microreactors

reactor	A-1	A-2	A-3	A-4	B
filter	none	glass	glass	glass	
grafting time, min	1	1	2	3	
V_{max}, nmol/min	0.15	0.18	0.13	0.25	0.14
K_m, mM	118	15.5	67.9	82.9	47.2
back pressure, MPa	15.8	3.4	7.6	7.3	9.1

monolith B. Both grafting time and light intensity have little effect on the V_{max} value, and no significant difference is detected for both types of the monolithic supports. In contrast, a much higher effect can be observed for K_m. Its value increases rapidly with the grafting time. For example, a 5-fold higher concentration of the substrate is necessary to generate the maximum velocity using the reactor based on support grafted for 3 min, as compared to that grafted for 1 min. Similarly, grafting in the absence of the glass filter also leads to a high value of K_m. This likely results from the increased amount of azlactone grafted at the pore surface, enabling the immobilization of a high quantity of trypsin. Since the loading density of enzyme is high, the substrate does not equally access all of the active sites. The other possible explanation is an enhanced multisite binding of the trypsin molecule on the surface with a high density of VAL units, leading to a change in the shape of the active site and, thus, to a decrease in its activity.

It should be also noted that the pressure required for pumping liquid through the grafted monolith at a defined flow rate increases as the time of VAL grafting increases (reactors A-2, A-3, and A-4, Table 2). This indicates that the pores of the monolith become increasingly more filled with a swollen layer of polyVAL. A higher extent of grafting is also observed when the polymerization reaction is carried out in the absence of the glass filter (reactor A-1, Table 2). The results indicate that optimal grafting is achieved after 1 min of irradiation through the glass filter (support A-2). The microreactor prepared using this grafted support exhibits both high V_{max}, and low K_m at the lowest flow resistance. The kinetic characteristics of this reactor are significantly enhanced, as compared to those of reactors prepared from the copolymerized support B.

Effect of Temperature on Enzymatic Activity. The proteolytic activity of trypsin depends on the temperature, with a maximum reported at a temperature of 37 °C.[24] Kinetic characteristics determined for trypsin immobilized on support A-2 (data not shown) confirm that our immobilized enzyme also exhibits its maximum activity at temperatures between 30 and 40 °C. Clearly, the immobilization process using the VAL chemistry does not appear to affect the basic properties of trypsin. This is in agreement with the results achieved with trypsin immobilized on other supports and using different chemistries.[25]

Monoliths in Nanoelectrospray Needles. The simplicity of the in situ method enables us to place monoliths directly in the nanoelectrospray tips using one of two possible approaches (Figure 1). In the first approach, the monolith is prepared in a capillary, and the nanoelectrospray needle is pulled afterward. This approach allows all of the chemistry, including polymerization, grafting, and trypsin immobilization, to be completed in the capillary prior to making the needle and prevents it from clogging or damage during the manipulations. The capillary with the monolith must be carefully aligned in the pulling instrument to fabricate the tip as close to the monolith as possible and create a minimum dead volume. The empty space of ~0.75 mm between the monolith and the tip shown in Figure 1a represents a volume of 15 nL, or 30% of the total volume of the monolith.

The other approach involves the preparation of the monolith directly in the tip of a preformed nanoelectrospray needle. Micrographs 1b and 1c show that the monolith protrudes to the very end of the tip and is clearly visible within the orifice of the needle with no dead volume. Since the tip is susceptible to damage, special care must be taken during the manipulations. Figure 1d shows a very well formed Taylor cone and ion beam that is produced from the monolithic tip.

Monoliths with Dual Function. The photolithographic-like grafting of the pore surface enables the preparation of monoliths containing several cocontiguous surface chemistries. For example, a monolith with two different functionalities is obtained in two simple steps: The first step consists of polymerization of mixture A that affords a hydrophobic monolith. In the second step, part of the capillary with the monolith inside is masked, the pores are filled with VAL solution containing benzophenone, and the capillary is irradiated with UV to achieve grafting of the pore

(24) (a) Dixon, M.; Webb, E. C. *Enzymes*; Academic Press: New York, 1958. (b) Lazdonski, M.; Delaage, M. *Biochim. Biophys. Acta* **1965**, *105*, 541−61.
(25) (a) Ding, L. H.; Li, Y.; Jiang, Y.; Cao, Z.; Huang, J. X. *J. Appl. Polym. Sci.* **2002**, *83*, 94−102. (b) Huang, X. L.; Catignani, G. L.; Swaisgood, H. E. *J. Biotechnol.* **1997**, *53*, 21−27.

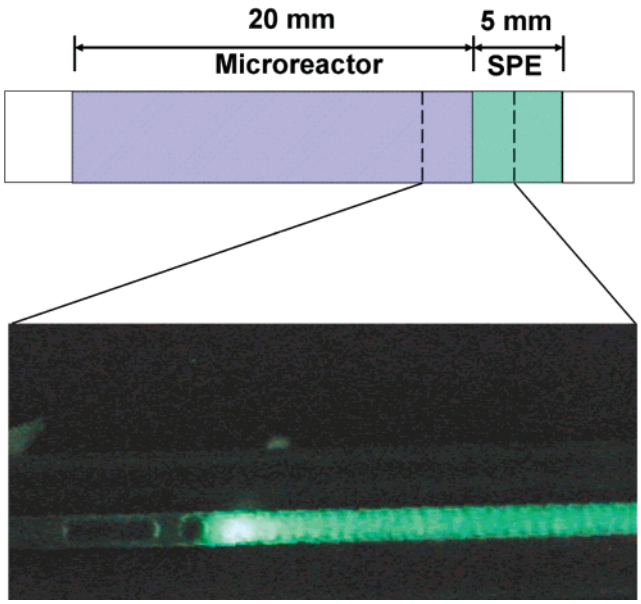

Figure 2. Scheme and fluorescence microscope image of the monolithic dual-function device used in the digest-SPE direction for digestion of labeled casein and capture of fluorescent peptides. Conditions: loading of 5 μL of 10 μg/mL BODIPY-labeled casein in 50 mmol/L Tris buffer (pH 8.0) at a flow rate of 0.5 μL/min followed by washing monolith with 10 μL of Tris buffer.

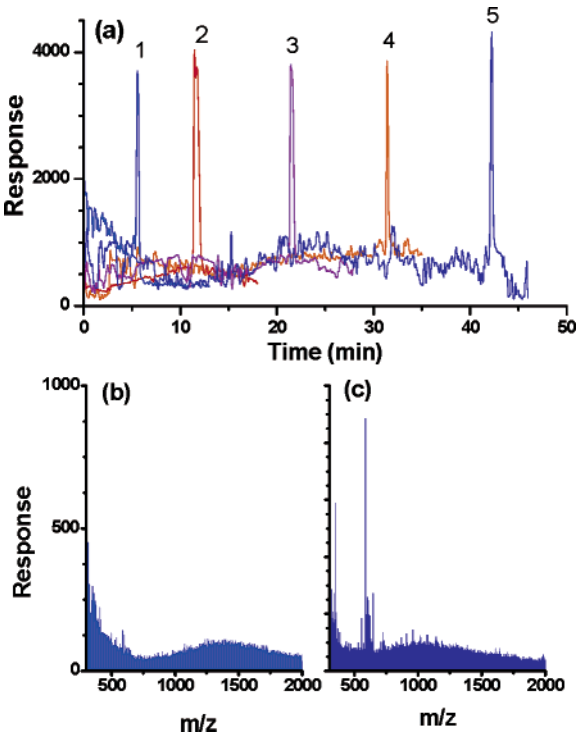

Figure 3. Total ion current monitoring of compounds eluted from monolithic dual-function device in SPE-digest direction for different loading volumes (a) and mass spectra of peaks 1 (b) and 5 (c). Conditions: flow rate of 0.5 μL/min, room temperature. Loading: myoglobin solution 19 pmol/μL; loaded volumes 2 (1), 5 (2), 10 (3), 15 (4), and 20 μL (5). Elution: acetonitrile 50 nL.

surface only in the unmasked part of the capillary. The following reaction with trypsin immobilizes the protein covalently only in the VAL-functionalized area. This path leads to a dual-function device shown schematically in Figure 2 that involves an unmodified hydrophobic part, which acts as a solid-phase extractor (SPE), and a microreactor with immobilized enzyme.

The dual function of the device was qualitatively demonstrated on digestion of BODIPY-labeled casein. This high molecular weight substrate contains intramolecularly quenched fluorescing moieties that fluoresce only after proteolytic digestion.[26] The micrograph of Figure 2 shows a part of the dual-function monolith located near the boundary of both chemistries. The casein solution is pumped through the enzyme reactor, and the resulting peptides are collected in the hydrophobic SPE. The monolith is subsequently washed with 10 μL of 50 mmol/L TRIS buffer solution to remove all unbound species. Clearly, the right part of the monolith containing immobilized trypsin exhibits no fluorescence, whereas the highest fluorescence, emanating from fluorescently labeled peptides, is observed in the part of the SPE device adjacent to the reactor. The intensity of fluorescence rapidly decreases with the distance from the boundary. The presence of captured fluorescent species confirms the digestive function of the device and the high fluorescence of peptides retained in the hydrophobic part of the monolith, even after washing proves its SPE ability.

Digestion of Myoglobin in Dual-Function Needles. The design of our dual-function microdevice is well-suited for the mapping of proteins present in dilute solutions through proteolytic digestion, followed by the identification of the resulting peptide masses using mass spectrometry. Myoglobin has often been used as a model to test systems that include a proteolytic digestion step.[14,27] To demonstrate the operational ability of our device for this application, a 19 pmol/μL aqueous myoglobin solution was pumped through the dual-function monolith. The compounds of interest were then released using a 50-nL plug of a strong solvent. Depending on the spatial location of the SPE component within the needle, pumping of the protein solution through the device may occur in both directions, that is, first through the SPE and then through the microreactor, or through the microreactor first, followed by the SPE device. We, therefore, tested the effect of the device configuration on its function.

Figures 3 and 4 show the monitored total ion current signals for the dual-function device for both configurations. The plots confirm the desirable signal increase observed after loading a higher sample volume. Although a 2-fold increase in the peak area is observed after concentration of myoglobin from 5 μL of solution, as compared to 2 μL, no further increase in peak area is seen for the larger volumes. It is also worth noting that the peaks recorded after using the device in digest-SPE configuration are significantly broader and split.

The concentration step also has a significant effect on the quality of the mass spectrum. For example, Figure 3 shows the mass spectra for myoglobin first preconcentrated from different volumes of solution, then released with 50 nL of acetonitrile, and digested. Clearly, as a larger volume of sample is loaded, the signal of the peptides increases, and the signal-to-noise ratio improves. This enables positive detection of a larger number of peptides,

(26) Jones, L. J.; Upson, R. H.; Haugland, R. P.; Panchuk-Voloshina, N.; Zhou, M. J. *Anal. Biochem.* **1997**, *251*, 144−52.

(27) (a) Ekstrom, S.; Onnerfjord, P.; Nilsson, J.; Bengtsson, M.; Laurell, T.; Marko-Varga, G. *Anal. Chem.* **2000**, *72*, 286−93. (b) Lazar, I. M.; Ramsey, R. S.; Ramsey, J. M. *Anal. Chem.* **2001**, *73*, 1733−39. (c) Litborn, E.; Emmer, A.; Roeraade, J. *Anal. Chim. Acta* **1999**, *401*, 11−19.

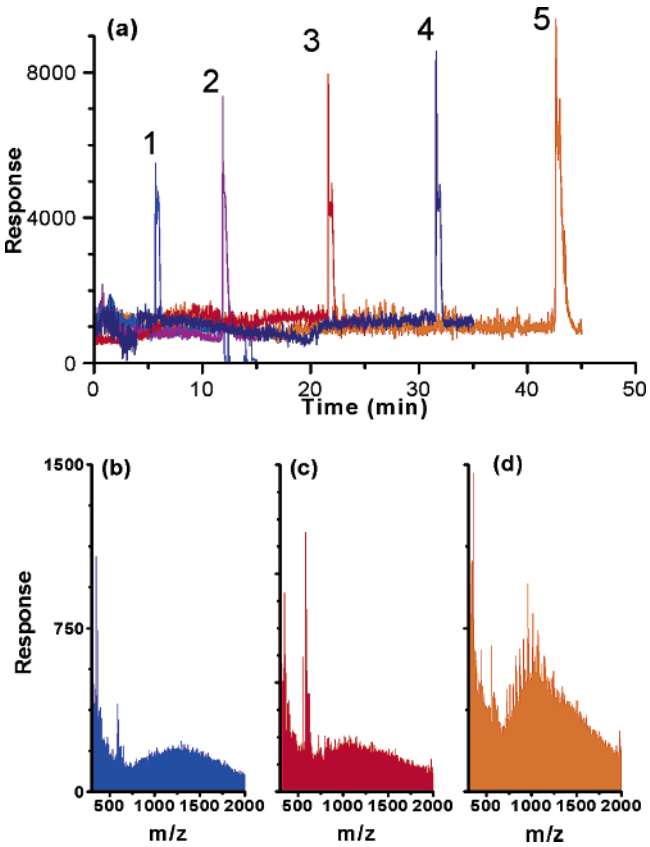

Figure 4. Total ion current monitoring of compounds eluted from monolithic dual-function device in digest-SPE direction for different loading volumes (a) and mass spectra of peaks 1 (b), 3 (c), and 5 (d). Conditions: Flow rate of 0.5 μL/min, room temperature. Loading: myoglobin solution 19 pmol/μL; loaded volumes 2 (1), 5 (2), 10 (3), 15 (4), and 20 μL (5). Elution: acetonitrile 50 nL.

which allows for higher sequence coverage and higher detection confidence. In contrast, much lower sequence coverage is observed in experiments with a single function device (enzyme reactor) operating without the preconcentration step regardless of the volume of protein solution.

The effect of sample volume on the mass spectra for the device used in the digest−SPE configuration is shown in Figure 4. A peak appears at ~1980 m/z for loading volumes of 15 and 20 μL, which corresponds to a large peptide (amino acid residues 79−96, 1 missed cleavage). Simultaneously, peaks of undigested myoglobin are also noticed at higher loadings.

Detailed analysis of the individual spectra collected from the peak of total ion current signals shown in Figures 3 and 4 reveals that the peak front is enriched in peptides, which elute first and precede the undigested myoglobin. This suggests that a displacement is occurring as a result of a stronger multipoint interaction of the undigested protein or its larger fragments with the pore surface of the concentrator. As a result, some separation of the peptides and undigested protein occurs, as manifested by the much broader and split nature of the total ion peak. The peaks are about twice as wide as those obtained in the SPE-digest configuration (Table 3).

Somewhat surprisingly, Table 3 also shows that a significant increase in sequence coverage is achieved for higher sample loadings, regardless of device configuration. Obviously, the immobilized enzyme should exhibit higher activity for more concentrated protein solutions, which would favor the SPE-digest configuration. However, the protein is eluted from the SPE section of the needle using an organic solvent, which is less suitable for the enzyme-catalyzed reaction and decreases overall enzymatic activity. In the opposite configuration, the enzyme operates under optimal conditions, thus alleviating the lower substrate concentra-

Table 3. Effect of Sample Loading and Percentage of Acetonitrile in the Eluent on Sequence Coverage of Digested Myoglobin for Dual-Function Device Operated in Different Flow Directions

	SPE → digestion[a]		digestion → SPE[a]	
volume loaded μL	seq. coverage %	peak width min	seq. coverage %	peak width min
no SPE	41	0.75	41	0.75
2	58	0.33	60	0.71
5	61	0.52	61	0.91
10	62	0.54	67	0.8
15	65	0.45	75	0.86
20	74	0.48	79	1.92

acetonitrile, %	sequence coverage, %	sequence coverate, %	
		1st peak	2nd peak
100	58	60	—[b]
80[c]	31	71	52
60[c]	13	65	45
40[c]	9	61	33

[a] The arrow indicates the direction of flow through the device. [b] All peptides eluted in a single peak. [c] Mixtures with water.

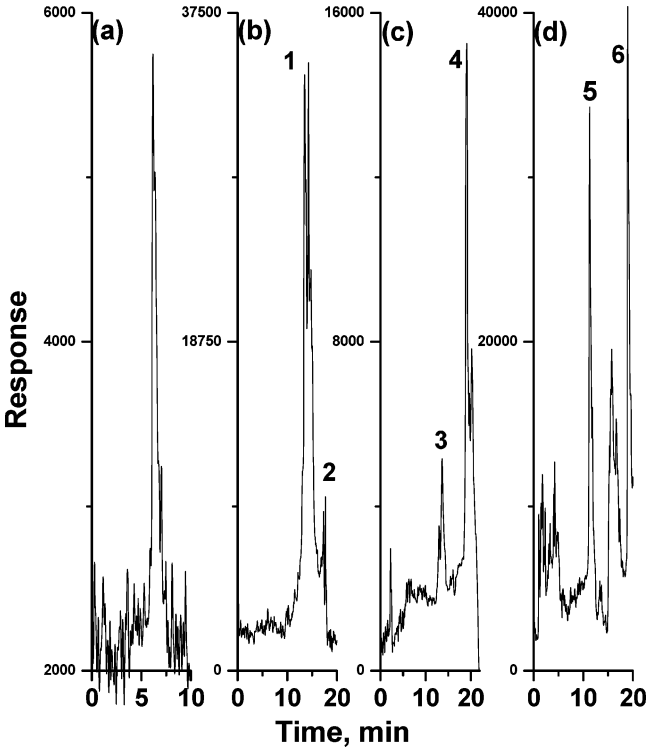

Figure 5. Total ion current monitoring of compounds eluted from monolithic dual-function device in digest-SPE direction using eluents with varying contents of acetonitrile. Conditions: Flow rate of 0.5 μL/min, room temperature. Loading: myoglobin solution 19 pmol/μL, volume 2 μL; Elution volume, 50 nL. Eluents: acetonitrile (a), acetonitrile−water 80:20 (b), 60:20 (c), and 40:60 (d).

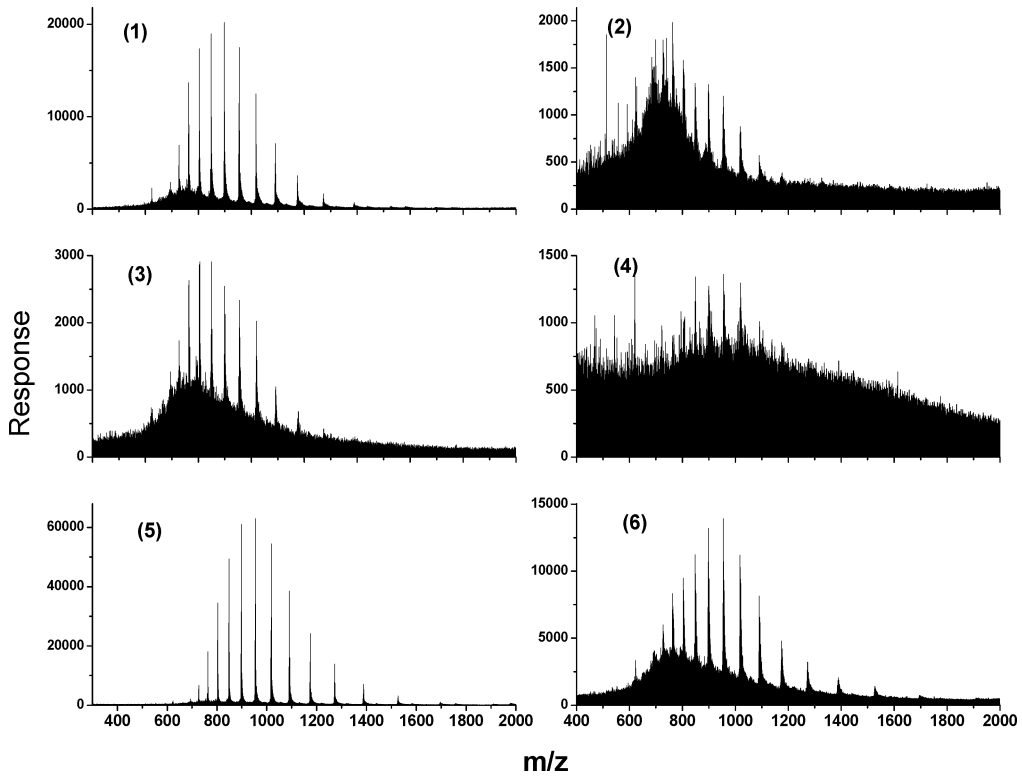

Figure 6. Mass spectra of compounds contained in numbered peaks of total ion current chromatograms shown in Figure 5.

tion. The peptides are released from the SPE by action of the organic solvent only after the digestion process has taken place.

Table 3 shows that the resulting sequence coverage for myoglobin is the same for use of the either directions. Obviously, the results obtained for other proteins might well differ, depending on their structure and size; however, in experiments unrelated to this research concerning the separation of proteins using monolithic capillary columns with chemistry identical to that of the SPE part of our dual-function devices, we have shown that even hydrophobic proteins, such as albumin and zein, can be readily eluted from the BuMA−EDMA monolith using pure acetonitrile with a recovery close to 100%. In addition, our previous work did not reveal any denaturation or loss of activity of trypsin, even after extended treatment with a variety of organic solvents typically used in reversed-phase elution mode.[14a] Recently, Slyzs and Schriemer also confirmed that the activity of immobilized trypsin is not affected by organic solvents.[28] This, together with the high protein recovery and the significantly enhanced concentration of proteins eluted in the narrow 50 nL band, appears to favor the SPE-digestion approach. Yet, a complete separation stage is likely to be included in the future designs of more complex devices. In this instance, however, the use of pure organic solvent to release the proteins would be impractical, since this approach may not be compatible with the subsequent chromatographic process. Therefore, alternative approaches to our current implementation of the SPE-digestion protocol will be required.

Release of Peptides from SPE Using Aqueous Acetonitrile. In addition to the use of pure acetonitrile, we tested the ability of acetonitrile−water mixtures to release the accumulated proteins and peptides from the SPE device. Although longer elution times are required with the aqueous eluents in the SPE-digest configuration, even a 40% aqueous solution of acetonitrile is capable of eluting the protein and peptides from the SPE device, demonstrating that the device tolerates a wide range of elution conditions. However, Table 3 shows that the sequence coverage rapidly decreases from 58 to only 9% as the percentage of water in the eluent increases. Simultaneously, an increase in the amount of undigested myoglobin is also observed. Since it is unlikely that the enzyme is less efficient in media richer in water, this must be due to a much less efficient release of protein from the SPE section of the needle and, thus, less substrate's reaching the enzymatic microreactor. The kinetics of the enzymatic reaction is significantly decreased at low protein concentrations, and more of the protein passes through the reactor undigested. Since a single peak with increased tailing is observed in the total ion trace, it is likely that the aqueous acetonitrile solutions release only the less tightly bound protein from the SPE device, while most of the strongly bound myoglobin remains adsorbed. This was confirmed by a subsequent release of residual protein using a pulse of pure acetonitrile. In this subsequent step, a high sequence coverage was again observed. These experiments indicate again that the SPE-digestion configuration is less suitable for the desired applications in more complex systems.

Figure 5 shows the total ion traces of the compounds released from the device used in the digest-SPE configuration. An increase in water content in the solvent affords traces with multiple peaks and a lower elution rate. This supports our assumption that separation of the protein and peptides occurs to some extent during their passage through the SPE device. The relative intensity of the two peaks also changes with decreasing strength of the eluting solvent. The intensity of the later eluting, protein-rich peak increases relative to the first peptide-rich peak. Obviously, the elution of protein in low-strength solvent is slow, whereas the peptides are released easily. Table 3 shows the

sequence coverage calculated for the two major peaks of the traces. Only a small decrease in sequence coverage from 71 to 61% is observed in the peak eluted first. In contrast, the sequence coverage calculated from spectra obtained with the protein peak decreases from 60 to only 33%. As shown in Figure 6, this peak, indeed, contains much of the undigested myoglobin and less peptides.

CONCLUSIONS

The site-selective UV-initiated photografting of monoliths through a mask is a powerful strategy to design new multifunctional devices for proteomic studies. It enables the preparation of numerous functional elements instrumental to the development of microanalytical systems. Our results demonstrate this approach on a dual-function device. This dual-function device significantly improves the sequence coverage for the digested protein, since much higher sample loading is possible. The use of our combined device was demonstrated in both directions, that is, SPE-digestion and digestion-SPE. Although both devices afforded very similar results, the former approach in its current implementation that requires use of organic solvent for the elution would be less practical in systems that would involve a chromatographic separation step. Since the preconcentration step remains a very desirable feature for the more complex systems we plan to fabricate in the future, we are currently studying alternative pathways to preconcentrators involving, for example, elution by changing the temperature.[29] Our approach has been demonstrated here using monoliths in capillaries. However, this work now opens a new avenue for the development of a number of functional microdevices with tailored properties within microfluidic chips, thus simplifying the construction of micrototal analytical systems (μTAS).

(28) Slyzs, G. W.; Schriemer, D. C. *Rapid Comm. Mass Spectrosc.* **2003**, *17*, 1044−1050.
(29) Peters, E. C.; Svec, F.; Fréchet, J. M. J. *Adv. Mater.* **1997**, *9*, 630−32.

ACKNOWLEDGMENT

This work was supported in part by the Office of Nonproliferation Research and Engineering of the U.S. Department of Energy under Contract no. DE-AC03-76SF00098. Support of this research by a Grant of the National Institute of General Medical Sciences, National Institutes of Health (GM-48364) is also gratefully acknowledged.

Received for review February 3, 2003. Accepted July 28, 2003.

AC034108J